USCAP

Check for updates

ARTICLE

Characterization of COVID-19-associated cardiac injury: evidence for a multifactorial disease in an autopsy cohort

Paul J. Hanson[1,2,12 ✉], Felicia Liu-Fei[1,12], Coco Ng[1], Taylor A. Minato[1], Chi Lai[2,3], Al Rohet Hossain[1], Rebecca Chan[3], Bobby Grewal[3], Gurpreet Singhera[2], Harpreet Rai[4], Jeremy Hirota[5,6,7,8], Daniel R. Anderson[9], Stanley J. Radio[10] and Bruce M. McManus[1,2,11]

As the coronavirus disease 2019 (COVID-19) pandemic evolves, much evidence implicates the heart as a critical target of injury in patients. The mechanism(s) of cardiac involvement has not been fully elucidated, although evidence of direct virus-mediated injury, thromboembolism with ischemic complications, and cytokine storm has been reported. We examined suggested mechanisms of COVID-19-associated heart failure in 21 COVID-19-positive decedents, obtained through standard autopsy procedure, compared to clinically matched controls and patients with various etiologies of viral myocarditis. We developed a custom tissue microarray using regions of pathological interest and interrogated tissues via immunohistochemistry and in situ hybridization. Severe acute respiratory syndrome coronavirus 2 was detected in 16/21 patients, in cardiomyocytes, the endothelium, interstitial spaces, and percolating adipocytes within the myocardium. Virus detection typically corresponded with troponin depletion and increased cleaved caspase-3. Indirect mechanisms of injury—venous and arterial thromboses with associated vasculitis including a mixed inflammatory infiltrate—were also observed. Neutrophil extracellular traps (NETs) were present in the myocardium of all COVID-19 patients, regardless of injury degree. Borderline myocarditis (inflammation without associated myocyte injury) was observed in 19/21 patients, characterized by a predominantly mononuclear inflammatory infiltrate. Edema, inflammation of percolating adipocytes, lymphocytic aggregates, and large septal masses of inflammatory cells and platelets were observed as defining features, and myofibrillar damage was evident in all patients. Collectively, COVID-19-associated cardiac injury was multifactorial, with elevated levels of NETs and von Willebrand factor as defining features of direct and indirect viral injury.

INTRODUCTION

As the severe acute respiratory syndrome coronavirus 2 (SARS-CoV-2) pandemic continues to ravage populations worldwide, our efforts to accumulate knowledge regarding the pathogenesis underlying clinical presentations of coronavirus disease 2019 (COVID-19) have matured. While initially considered primarily a respiratory disease, COVID-19 has become associated with myocardial injury, with reports of cardiac damage in over 20% of patients[1]; early studies from Wuhan indicate 51.2% increase in-hospital mortality among those with cardiac injury[2]. Magnetic resonance imaging has further determined 78% of unselected, recovered COVID-19 patients to have lasting cardiovascular effects[3]. COVID-19-associated cardiac damage may manifest as myocarditis, cardiogenic shock, thrombosis, or ischemic injury, reflected in impaired left ventricular ejection fraction and elevated serum troponin[1,4–11]. Clinical risk factors include male sex, advanced age, and comorbidities such as hypertension, obesity, and diabetes[12].

Whether mechanisms such as direct viral cardiotoxicity, immune-thrombotic changes, dysregulated immune response, or a combination of such are responsible for cardiac injury have yet to be fully elucidated. Still, recent studies have touched on the matter. On the basis of clinical and histological evidence, potential mechanisms of injury include (1) direct viral insult[13] or (2) indirect damage to the heart due to hypoxemia as a result of acute respiratory distress syndrome, (3) elevated thromboembolic risk[4,14–16], and (4) COVID-19-associated cytokine storm syndrome (CSS) and inflammation-mediated tissue injury[17,18].

To date, findings of viral infection of the heart have been limited. In vitro evidence suggests that SARS-CoV-2 preferentially targets cardiomyocytes[19], consistent with high angiotensin-converting enzyme 2 (ACE2) expression (the primary receptor) on cardiomyocytes[20,21]. However, ACE2 expression alone may not account for observable tissue tropism[22], and clinical evidence of cardiomyocyte infection is sparse. Increasing evidence suggests that endothelial dysfunction and thromboembolic disease

[1]UBC Centre for Heart Lung Innovation, Vancouver, BC, Canada. [2]UBC Department of Pathology and Laboratory Medicine, Vancouver, BC, Canada. [3]Department of Pathology and Laboratory Medicine, Providence Health Care – St. Paul's Hospital, Vancouver, BC, Canada. [4]Department of Pathology and Molecular Medicine, McMaster University, Hamilton, ON, Canada. [5]Department of Biology, University of Waterloo, Waterloo, ON N2L 3G1, Canada. [6]Michael G. DeGroote Institute for Infectious Disease Research, McMaster University, Hamilton, ON L8S 4K1, Canada. [7]McMaster Immunology Research Centre, McMaster University, Hamilton, ON L8S 4K1, Canada. [8]Firestone Institute for Respiratory Health – Division of Respirology, Department of Medicine, McMaster University, Hamilton, ON L8N 4A6, Canada. [9]Division of Cardiovascular Medicine, Department of Internal Medicine, University of Nebraska Medical Center, Omaha, NE, USA. [10]Department of Pathology and Microbiology, University of Nebraska Medical Center, Omaha, NE, USA. [11]PROOF Centre of Excellence, Vancouver, BC, Canada. [12]These authors contributed equally: Paul J. Hanson, Felicia Liu-Fei. ✉email: Paul.Hanson@hli.ubc.ca

P.J. Hanson et al.

815

Table 1. Summary of COVID-19 patient demographics, laboratory results, pre-existing conditions, histopathological and macroscopic pathological features.

	COVID-19 patients ($n = 21$)
Demographics	
Age (years)	64.3 (35–85)
Male sex	17 (81%)
BMI (kg/m^2)	32.7 (22.0–48.0)
Ventilator	20 (95.2%)
Lab results	
Platelets (10E3/µL)	232 (62–365)
INR	1.5 (1.0–2.6)
PTT (s)	40.9 (22.7–114.4)
D-dimer (ng/mL)	1222 (<215–3723)
Troponin (ng/mL)	0.08 (<0.04–0.13)
Pre-existing conditions	
Hypertension	16 (76%)
Hyperlipidemia	11 (52%)
Coronary artery disease	5 (24%)
Diabetes mellitus type II	9 (43%)
Chronic kidney disease	6 (29%)
Gastroesophageal reflux disease	5 (24%)
Histopathological features	
Fibrosis	9 (43%)
Edema	19 (90%)
Borderline myocarditis	19 (90%)
Monocyte hypertrophy	15 (71%)
Myocytolysis	10 (48%)
Blood vessel congestion	10 (48%)
Thrombosis	4 (19%)
Hemorrhage	4 (19%)
Pericarditis	2 (9.5%)
Macroscopic pathological features	
Average heart weight (g)	447 (282–671)
Right ventricular hypertrophy	6 (29%)
Left ventricular hypertrophy	10 (48%)
LAD narrowing (%)	54 (0–90)
LCA narrowing (%)	48 (0–90)
RCA narrowing (%)	49 (0->90)
Right ventricular dysfunction	8 (38%)
Left ventricular dysfunction	5 (24%)
Small vessel thrombi	4 (19%)
Lymph inflammation (myocardium)	4 (19%)
Lymph inflammation (epicardium)	2 (10%)
Acute myocardial infarction	3 (14%)
Hemorrhagic myocardial infarction	6 (29%)

LAD left anterior descending, *LCA* left coronary artery, *RCA* right coronary artery.

affecting the macro and microvasculature play a significant role in COVID-19-associated cardiac (and multi-organ) injury[16,23–25]. The resultant damage, either by direct virus injury or thrombus formation and ischemia, is postulated to participate in triggering cytokine storm during the late phase of COVID-19[26], characterized by significant elevations in serum IL-6[18,24,27] and associated with increased morbidity and mortality. Histological analyses of COVID-19 patients demonstrated significant inflammation, including neutrophils and lymphocytes present in the lungs, heart, kidneys, liver, and brain up to 6 weeks post onset of symptoms, indicative of an autonomous maladaptive immunity[28]. However, the inflammatory phenomenon and the contribution of CSS are still the subjects of controversy[29].

Collectively, studies to date regarding COVID-19-associated cardiac injury indicate distinct phases and phenotypes of injury though incomplete regarding the understanding of the mechanisms and key factors involved. Thus, this study's objectives are to better delineate the clinical course, pathophysiology, and mechanism(s) of COVID-19-associated cardiac injury. To this end, we analyzed (1) direct viral injury and associated myocyte damage, (2) presence of macro/micro thrombosis and factors involved in endothelialitis, thrombosis, and angiogenesis, and (3) factors involved in cytokine storm, immune-mediated injury, and immune cell populations in twenty-one consecutive autopsy decedents. We compared our findings to other forms of virus-associated heart failure attributable to influenza B, coxsackievirus B3 (CVB3), adenovirus 2 (AAV2), and hepatitis C virus (HCV) as well as to healthy controls and clinically matched controls (CMC) to shed light on the mechanisms of COVID-19-associated cardiac injury.

MATERIALS AND METHODS
COVID-19 patients
Cardiac tissues from 21 consecutive, fatally ill COVID-19+ patients were collected at the University of Nebraska Medical Center (Omaha, NE) between April and December 2020. All tissues were collected under ethically approved guidelines (H05-50004, H15-40080) in accordance with the Code of Ethics of the World Medical Association (Declaration of Helsinki). For all human subjects, informed consent was obtained via a written waiver before individuals were deceased. All studies were performed on tissues from patients with diagnosed COVID-19 as indicated by active SARS-CoV-2 infection via nasopharyngeal swab and positive PCR test. Anonymized, hematoxylin and eosin (H&E) stained tissue sections were assessed by cardiovascular pathologists (B.M.M., S.J.R., and C.L.) blinded to diagnosis to delineate the histopathological findings related to direct viral injury, thrombus presence, and inflammation. Clinical and histopathological characteristics are summarized in Table 1. Regions of pathological interest were selected and used to generate a custom, single-slide tissue microarray (TMA) (see Tissue Microarray Design).

Control patients
All subsequent molecular assays and analyses were performed in parallel on corresponding control tissues from patients with clinically diagnosed, in situ hybridization (RNAscope®)-confirmed virus-associated heart failure ((HCV ($n = 3$), CVB3 ($n = 3$), influenza B ($n = 3$), AAV2 ($n = 3$)), COVID-19 CMC ($n = 14$) and healthy controls ($n = 10$) (see Supplementary Table 1C). Cardiac tissues from viral control patients were obtained from diseased transplant hearts and autopsy, tissues from CMC were obtained from transplant, and tissues from normals were obtained from autopsy. To the degree possible, patients were age- and sex-matched with COVID-19 patients (see Supplementary Table 1C).

Patient clinical information
For all patients, de-identified clinical information, including demographic, clinical status variables, comorbidities, and blood laboratory results, were paired with molecular analysis data made available under ethically approved guidelines.

In situ hybridization via RNAscope®
In situ hybridization was conducted on 4-µm paraffin sections using RNAscope® 2.5 HD Red Assay. RNAscope® probes detected the SARS-CoV-2 S gene encoding spike protein sense strand (ACD V-nCoV2019-Sense). SARS-CoV-2-positive patient lung tissue was used as positive control tissue. In situ hybridization via RNAscope® detected the replicative strand of CVB3,

Laboratory Investigation (2022) 102:814 – 825

SPRINGER NATURE

influenza B, HCV, and AAV2 in patients with pathologist-confirmed viral myocarditis at transplant/explant or autopsy that were utilized as control tissues.

Tissue microarray design

Two identical TMAs were designed, each consisting of heart tissue from regions of pathological interest, determined by cardiac pathologist examination, from SARS-CoV-2, CVB3, influenza B, HCV, AAV2 patients, CMC, and healthy controls. The TMAs included 21 COVID-19 patients, 3 CVB3, influenza B, HCV, AAV2 patients each, 14 COVID-19 CMC patients, and 10 non-infected control patients. A TMA instrument (TMA Master II, 3D Histech, Budapest Hungary) extracted tissue cores 2 mm in diameter corresponding to regions of pathological significance in the left and right ventricles and ventricular septum from individual FFPE blocks and transferred the cores into the custom-designed TMA. All subsequent immunohistochemical (IHC) staining was conducted using the TMA.

Tissue fixation, processing, histological and immunohistochemical staining

All patient cardiac tissues were fixed in 10% neutral buffered formalin (Fisher) for at least 24 h and subsequently embedded in paraffin blocks. Four-μm sections from the TMA were placed onto glass slides for histological (H&E) and IHC staining. IHC staining was performed on a Roche Ventana BenchMark Ultra IHC System (Optiview DAB detection) with heat-induced epitope retrieval using Roche CC1 (high pH) solution or Leica Bond RX (red bond polymer staining) automated stainers and counterstained with hematoxylin. To quantify our three postulated mechanisms of SARS-CoV-2-associated cardiac injury, we conducted staining for (1) direct viral injury (IHC staining for SARS-CoV-2 spike protein and RNAscope® in situ hybridization for SARS-CoV-2 spike protein sense strand) and associated myocyte damage (cleaved caspase-3 and troponin-I), (2) presence of macro/micro thrombosis (histological observation, CD61) and factors involved in endothelialitis, thrombosis and angiogenesis[30] Von

Willebrand factor (vWF), fibrinogen, CD31 (platelet endothelial cell adhesion molecule) and (3) factors involved in cytokine storm, immune-mediated injury and immune cell populations (CD45 (leukocyte common antigen), CD4 (helper T cell), CD8 (cytotoxic T cell), CD68 (macrophage), IL-6, C4D (complement), and citrullinated histone 3 (CitH3) and myeloperoxidase (MPO) as markers of neutrophil extracellular traps NETs)) (Fig. 1). All tissues from all patients were stained for every marker uniformly. Briefly, all staining was quantified using computer-aided image analysis (see Data analysis below).

Data analysis

Protein expression was quantified via ImageScope™, a computer-aided image analysis software used to detect DAB and Leica Bond RX red polymer staining for the respective indicated proteins. All values were normalized to the average value of normal, healthy controls per signal ($n = 10$). Individual groups were analyzed via Student's t-test in comparison to normal. The results are expressed as means of at least three patients per patient group (i.e., CVB3, HCV, etc. $n = 3$ or more). A P value of less than 0.05 was considered statistically significant. Asterisks represent significant differences between groups.

RESULTS
COVID-19 patient demographics

The mean age of COVID-19 decedents was 64 years (range 35–85), with 19% of patients being female. All patients except one required ventilation and 67% of patients had elevated D-dimer levels (>500 ng/mL), indicative of thrombosis. The average troponin-I level of patients during hospitalization was 0.08 ng/mL, and individual measurements are summarized in Supplementary Table 1A. All troponin levels were measured via the Beckman Coulter Dxi 800 immunoassay system. The most common
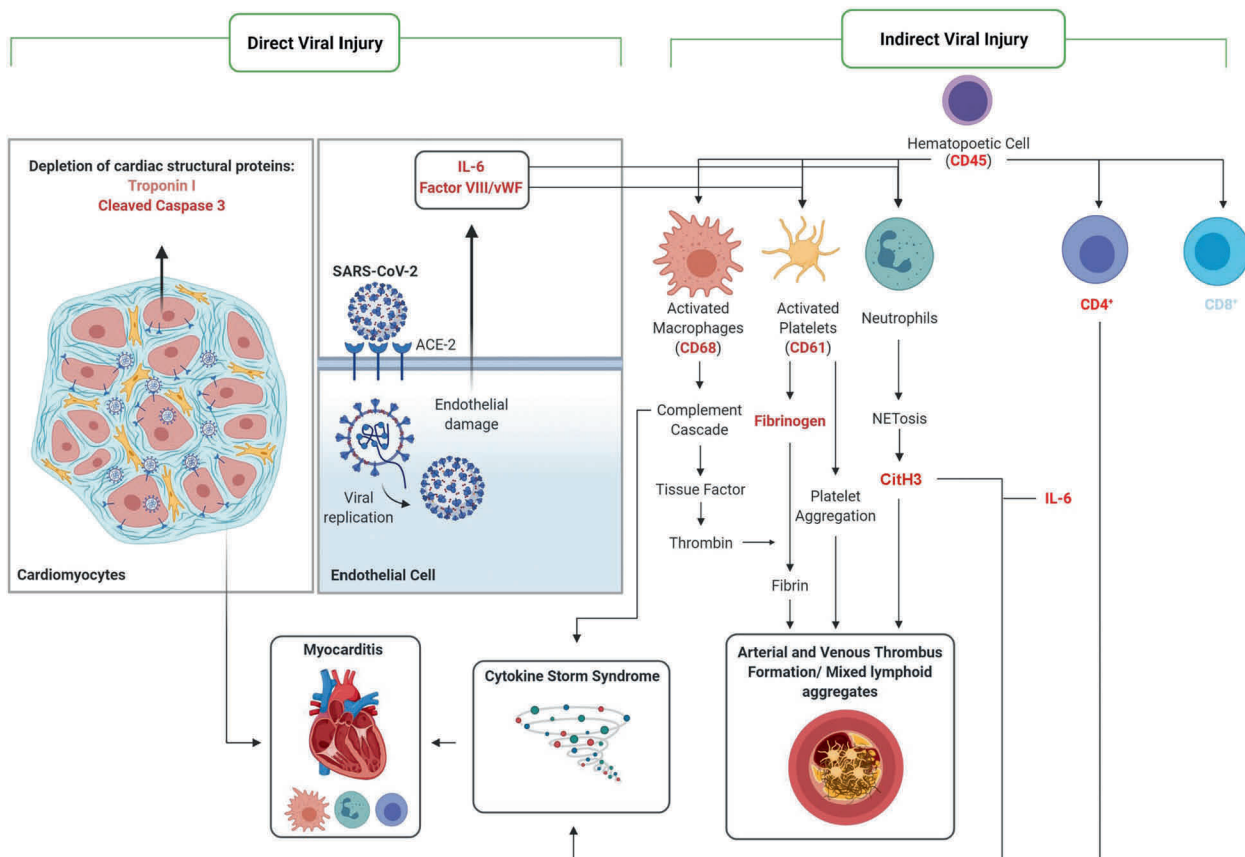

Fig. 1 Summary of mechanism(s) of COVID-19-associated myocardial injury. Proteins of interest ((shown in red (increased expression) and blue (decreased expression) text)) stained via IHC and quantified in cardiac tissues of COVID-19-positive decedents relative to normal control tissue.

comorbidities were hypertension (76%), hyperlipidemia (55%), and type II diabetes (40%). However, comorbidities were largely varied (Supplementary Table 1A) and also included coronary artery disease, chronic kidney disease, and deep vein thrombosis. The majority of patients (16/21) did not have previous clinical cardiac diagnoses, although cases of takotsubo cardiomyopathy, transmural acute myocardial infarction, and hemorrhagic myocardial infarction were reported (Supplementary Material 1A). Notably, one patient was the recipient of a heart and lung transplant. In our cohort, 81% of individuals met the criteria for being overweight or obese.

Clinical comparison of patient groups
Compared to our group of CMC, the mean of the COVID-19 cohort was obese, while CMC were overweight (BMI: 32.7 vs 26.4 for COVID-19 vs controls, $p = 0.005$). Due to a limited range of selection for control patient samples, certain demographics including age (64.3 vs 65.6, $p = 0.711$), sex (81 vs 79% male, $p = 0.886$), and various comorbidities including hypertension (76.2% vs 85.7%, $p = 0.498$) and diabetes (42.9% vs 28.6%, $p = 0.398$) varied slightly (Supplementary Table 1C). The heart weights between patient groups also differed slightly, with COVID-19 hearts having an average mass of 447 g and CMC hearts averaging 512 g ($p = 0.057$) (Table 1 and Supplementary Table 1D). χ^2 tests and two-sample t-tests were used to measure statistical significance.

Patient pathological findings
Upon analysis of COVID-19 patient cardiac tissue by expert cardiac pathologists (B.M.M., S.J.R., and C.L.) blinded to diagnoses, several notable findings were observed. Histopathological evidence meeting the "Dallas criteria" for borderline myocarditis (inflammation without associated myocyte injury) was observed in 19/21 patients. In addition, we found that 90% (19/21) of patients had interstitial myocardial edema, 71% had myocyte hypertrophy, and 48% had features of myocytolysis. Moreover, prominent congestion of the blood vessels (with and without thrombosis) was noted in 19% (4/21) of decedents. The average heart weight was 447 g and multiple patients had evidence of right (6/21) and left (10/21) ventricular hypertrophy, right (8/21) and left (5/21) ventricular dysfunction, and acute (3/21) and hemorrhagic myocardial infarction (6/21) (Table 1).

Detection of SARS-CoV-2 in hearts of critically ill COVID-19 patients
RNAscope® in situ hybridization was utilized to detect the sense strand coding for the SARS-CoV-2 spike protein and IHC staining was used to detect the spike protein. SARS-CoV-2 sense strand targeting the spike protein region was detected to varying degrees in the hearts of most decedents ($n = 16$) at autopsy, indicating transcriptionally active virus within the heart (Fig. 2G). SARS-CoV-2 spike protein was also detected via IHC in the hearts of 16/21 decedents (Fig. 2H). In general, viral RNA was sparse, focal, and patchy in distribution and was localized within cardiomyocytes, the interstitium, adipocytes within the visceral epicardium, and percolating adipocytes within the myocardium (Fig. 3).

Direct virus-mediated cardiac injury in COVID-19 patients
Beyond findings on routine H&E stained microscopy, myofibrillar damage was evident upon histological evaluation in all COVID-19 patients, regardless of whether they presented clinically with heart failure, based on levels of troponin-I and caspase-3 obtained through quantitative image analysis (Figs. 4 and 7). Tissue levels of troponin-I were depleted in many COVID-19 patients relative to normal and CMC, indicative of structural, sarcomeric damage to the cardiomyocytes (Fig. 4). Though troponin is a non-specific marker of cardiac injury, these results in conjunction with viral presence in regions of troponin depletion could indicate that the virus likely contributed to this structural damage. Accordingly, the majority (16/21) of patients in our cohort are proposed to exhibit direct viral injury as indicated by viral presence, depleted cardiomyocyte structural proteins, and significant levels of cleaved caspase-3 as compared to CMC, normals, and viral myocarditis controls (4.92-fold, 5.59-fold, 1.81-fold, respectively), suggestive of cellular apoptosis. Although also significant in areas of damage and edema, inflammation could not be directly attributed to direct viral damage as the viral presence was sparse in distribution.

Presence of arterial and venous thrombi, vasculitis, and enhanced angiogenesis—a feature unique to COVID-19-associated injury
Thrombi in macro and microvasculature were notable in the hearts of 19.1% (4/21) of critically ill COVID-19 patients in our cohort (Fig. 3). Compared with other forms of virus-associated heart failure, venous and arterial thrombi were notable features of COVID-19 (Fig. 5). CD61, indicative of platelet activation, was significantly enhanced among COVID-19 patients (5.56-fold relative to normal), along with venous and arterial thrombi identified histologically. In addition, fibrinogen (CMC: 2.56-fold, normal: 1.33-fold, viral myocarditis: 1.28-fold) and vWF (CMC: 3.59-fold, normal: 4.71-fold, viral myocarditis: 2.21-fold) were significantly increased among COVID-19 patients relative to controls indicating coagulopathy. Increases in CD61, vWF, and fibrinogen were common only among COVID-19 patients when compared to other viral controls. As indicated by greatly enhanced CD31 expression (CMC: 11.04-fold, normal: 2.06-fold, viral myocarditis: 3.83-fold), angiogenic activity was also significant and unique among COVID-19 patients relative to controls and all other etiologies of viral myocarditis, suggestive of a COVID-19-specific process. In most instances, thrombi were associated with vasculitis, with inflammation predominantly consisting of macrophages, neutrophils, and occasional T cells (Fig. 5).

Enhanced expression of NETs in the myocardium of critically ill COVID-19 patients
Significant increases in NETs as indicated by MPO (5.38-fold relative to CMC) (Fig. 4) were observed diffusely in the cardiac tissue of all COVID-19 patients within our cohort. MPO presence in COVID-19 patients was also found to be increased when compared to other cardiotropic viruses (3.20-fold), and healthy normals (3.65-fold). We further observed a unique, positive relationship between SARS-CoV-2 spike protein expression and MPO expression in the myocardium. NETs, as detected by MPO, were present within thrombi and in the surrounding vasculature (Fig. 5) and interspersed throughout the myocardium in regions of myocardial injury and was associated with troponin depletion fibrinogen and vWF deposition (Fig. 4). To further corroborate our findings of NETs, we performed CitH3 staining, which was upregulated when compared to CMC (1.94-fold), cardiotropic viruses (2.07-fold), and healthy normals (4.47-fold). In 18/21 COVID-19 patients, CitH3 was upregulated.

COVID-19-associated cardiac inflammation: myocarditis, pericarditis, and lymphocytic aggregates
COVID-19-associated myocarditis was distinctly less severe in comparison to control viral myocarditis patients who exhibited severe acute and fulminant myocarditis, with transmural inflammation in a number of instances. However, borderline myocarditis was observed in 19/21 COVID-19 decedents. Inflammatory infiltrate was a mix of predominantly mononuclear cells consisting of macrophages as assessed by CD68 expression (CMC: 5.24-fold, normal: 1.50-fold, viral myocarditis: 1.07-fold) and CD4 (CMC: 3.39-fold, normal: 3.77-fold, viral myocarditis: 3.35-fold) positive T cells with occasional polymorphonuclear leukocytes (neutrophils and rare eosinophils) detected within areas of edema and myocardial damage and within the interstitium as found from pathologist H&E routine microscopy review (Supplementary Fig. 2).
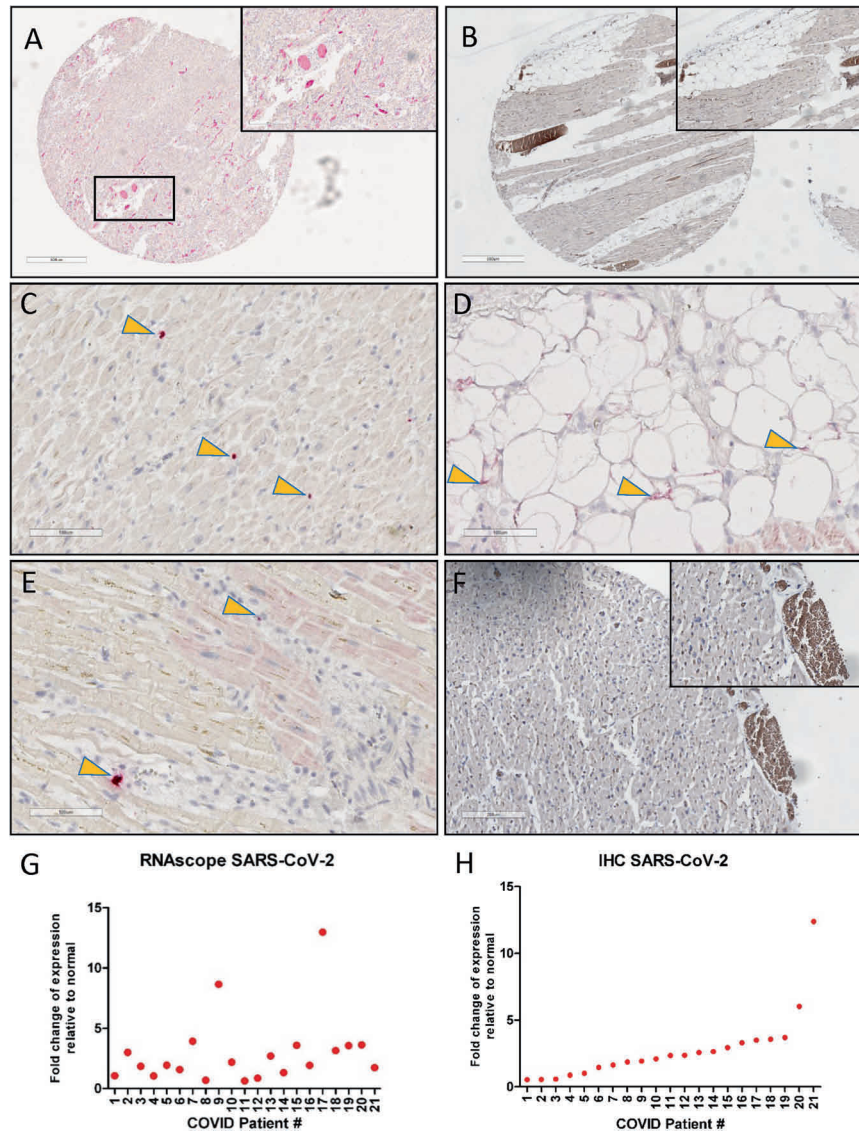
Fig. 2 Detection of SARS-CoV-2 sense strand RNA and spike protein in the myocardium. Representative images of SARS-CoV-2 sense strand spike protein within the interstitium (**E**), within blood vessels (**A**), within dying cardiac myocytes (**C**), and within percolating myocardial adipose tissue (**D**). SARS-CoV-2 spike protein expression was detected in blood vessels (**B**) and inflammatory infiltrates regions (**F**), where lipofuscin was also detected in the cardiomyocytes. Graphical representation of SARS-CoV-2 spike protein expression (**H**) and replicative strand expression (**G**) in the hearts of 21 COVID-19 patients. Yellow arrows indicate regions of viral positivity.

Furthermore, C4d (CMC: 4.44-fold, normal: 3.78-fold, viral myocarditis: 3.36-folds), a complement protein, IL-6, a proinflammatory cytokine, (CMC: 10.49-fold, normal: 4.08-fold, viral myocarditis: 1.56-fold), and CD45 (CMC: 4.37-fold, normal: 1.95-fold, viral myocarditis: 1,09-fold), a marker of hematopoietic cells, were all found to have increased expression in the heart when compared to CMC, while CD8-positive T cells were diminished in the majority of patients compared to comorbidity matched controls (CMC: 0.63-fold, normal: 1.55-fold, viral myocarditis: 0.31-fold). In addition to myocarditis, cardiac inflammation in the COVID-19 patients was commonly associated with vasculitis (Figs. 2 and 5) and also pericarditis, with prominent inflammation in the visceral epicardium (Fig. 3G) and surrounding adipose tissue. Adipocytes were commonly associated with inflammation both in the visceral epicardium as well as in percolating adipose tissue within the myocardium, a feature common in obese individuals. A lymphocytic lesion (resembling a "Quilty" lesion seen in transplanted allograft hearts) lining the right ventricular endocardium was observed in one patient (see Supplementary Fig. 1). The lesion consisted primarily of a lymphocytic infiltrate, with rare macrophages present and extended slightly into the myocardium with myocyte destruction noted by localized depletion of troponin-I. Large luminal masses of inflammatory cells interspersed with platelets were detected in the right ventricle of one patient and the left ventricle of another patient in our COVID-19 patient cohort (Fig. 6). Detection of SARS-CoV-2 was not present in myocarditic lesions, although it was sparsely detected in luminal masses of mixed inflammatory cells detected in the RV of one patient and LV of another patient (Fig. 6). SARS-CoV-2 expressed along the endothelium, and an inflamed artery due to COVID-19-associated damage within the myocardium was also observed (Fig. 5). All IHC signals quantified for COVID-19 patients are summarized in the heatmap (Fig. 7).

DISCUSSION
This study characterizes the pathological features of COVID-19-associated cardiac injury in relation to three primary proposed
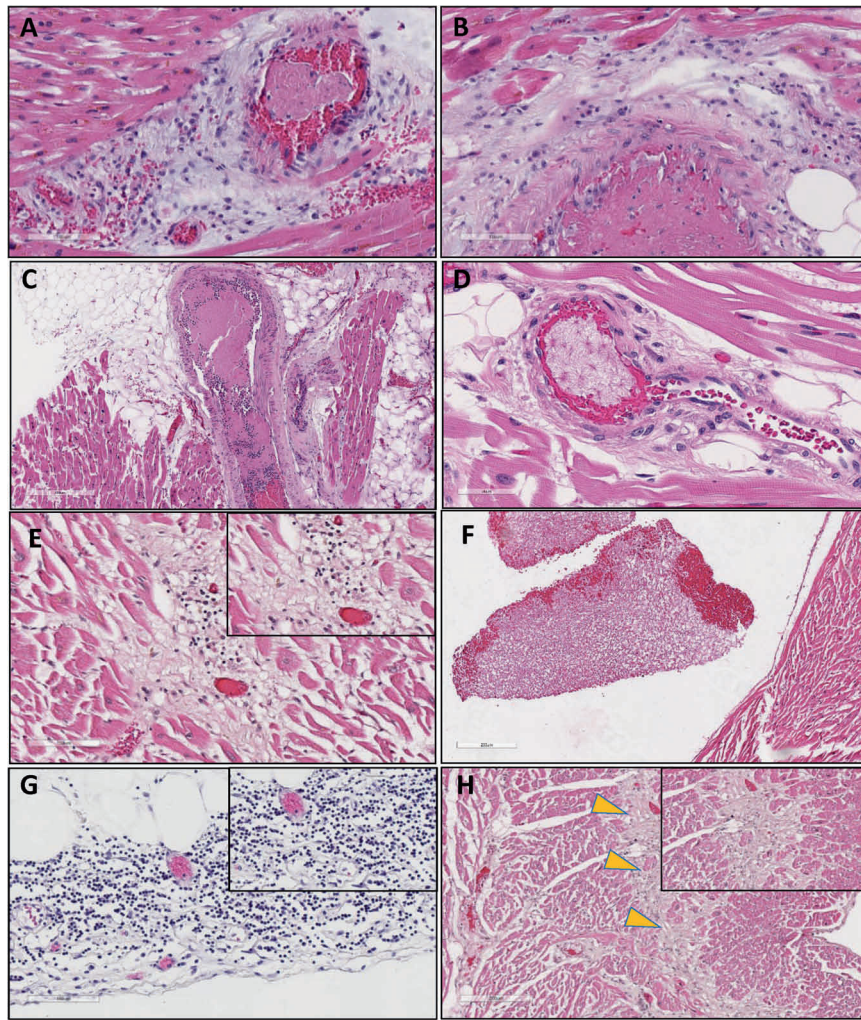
Fig. 3 Characteristic histopathologic features of COVID-19-associated cardiac injury in critically ill patients. Hematoxylin and eosin staining of representative cardiac injury among critically ill COVID-19 patients. COVID-19 patients exhibited pathological features of direct and indirect viral injury of the heart. Upper panels (**A–D**) are characteristic arteriole (**A, B**) and venous (**C, D**) thrombus. Regions of myocarditis from a COVID-19-positive decedent are shown in **E**, characteristic fibrin-rich thrombus and cardiomyocyte injury in COVID-19 patient (COVID-19) with history of myocardial infarction (**F**), mononuclear predominant inflammatory infiltrate within the visceral epicardium, and surrounding adipocytes (**G**) and a zone of ischemia (yellow arrows) in a patient with COVID-19-associated acute coronary syndrome demonstrating late healing with pigmented macrophages (**H**). Images **A, C, F,** and **G** are shown at ×10 magnification, **B** and **E** are shown at ×20 magnification, **D** is shown at ×40 magnification, and **G** is shown at ×4 magnification.

mechanisms: (1) direct viral injury, (2) vasculitis, endotheliaitis, and resultant thrombotic-mediated injury and (3) cytokine storm/immune-mediated injury (Fig. 1). Our results provide evidence of all three processes occurring to varying degrees in a cohort of 21 consecutive COVID-19 decedents. We compared histopathologic features of the myocardium of COVID-19 patients to common etiologies of virus-associated heart failure patients, clinically matched, and healthy controls. Herein, we provide evidence of direct viral injury to the myocardium by SARS-CoV-2 within cardiomyocytes[31] and confirm reports of virions within the interstitium[13]. In 16/21 patients, SARS-CoV-2 was sparsely distributed within the heart, suggestive of additional mechanisms of COVID-19-associated cardiac injury. Our results can be compared to a systematic review of cardiac autopsies from COVID-19 decedents, where SARS-CoV-2 was detected within the myocardium of 50/105 hearts (47%)[32]. We additionally provide, to our knowledge, the first evidence of SARS-CoV-2 infection of percolating adipocytes within the myocardium in autopsy patients (Fig. 2). The finding of SARS-CoV-2 infection of percolating adipocytes within the myocardium (Fig. 2D) is consistent with

the hypothesis proposed by Cinti et al.[33] that SARS-CoV-2 infects adipocytes (which express high levels of the SARS-CoV-2 receptor ACE2 in murine models of obesity[34]) and with reports of increased risk and severity of the clinical course of COVID-19 in obese individuals[35,36]. Despite randomized and unbiased selection of autopsy patients, the majority (78%) of our patients were overweight or obese; our findings are consistent with obesity being associated with severe outcomes of COVID-19 and provide mechanistic evidence of SARS-CoV-2 infection of adipose tissue.

In addition to direct viral-mediated injury, we report indirect injury attributable to immune-ischemic damage in the hearts of our COVID-19 decedents (Fig. 3). Recent research has revealed an intriguing correlation between thrombosis and SARS-CoV-2 infection, which to date has been primarily focused on the lungs[37]. Alveolar capillary microthrombi were especially prevalent in COVID-19 patients, present at nine times the amount compared to influenza patients[37], consistent with levels of CD61 in our COVID-19 patient hearts in comparison to influenza-induced heart failure (4.76-fold higher) (Fig. 4). Additional reported features of COVID-19 patient lungs include severe endothelial injury, which is
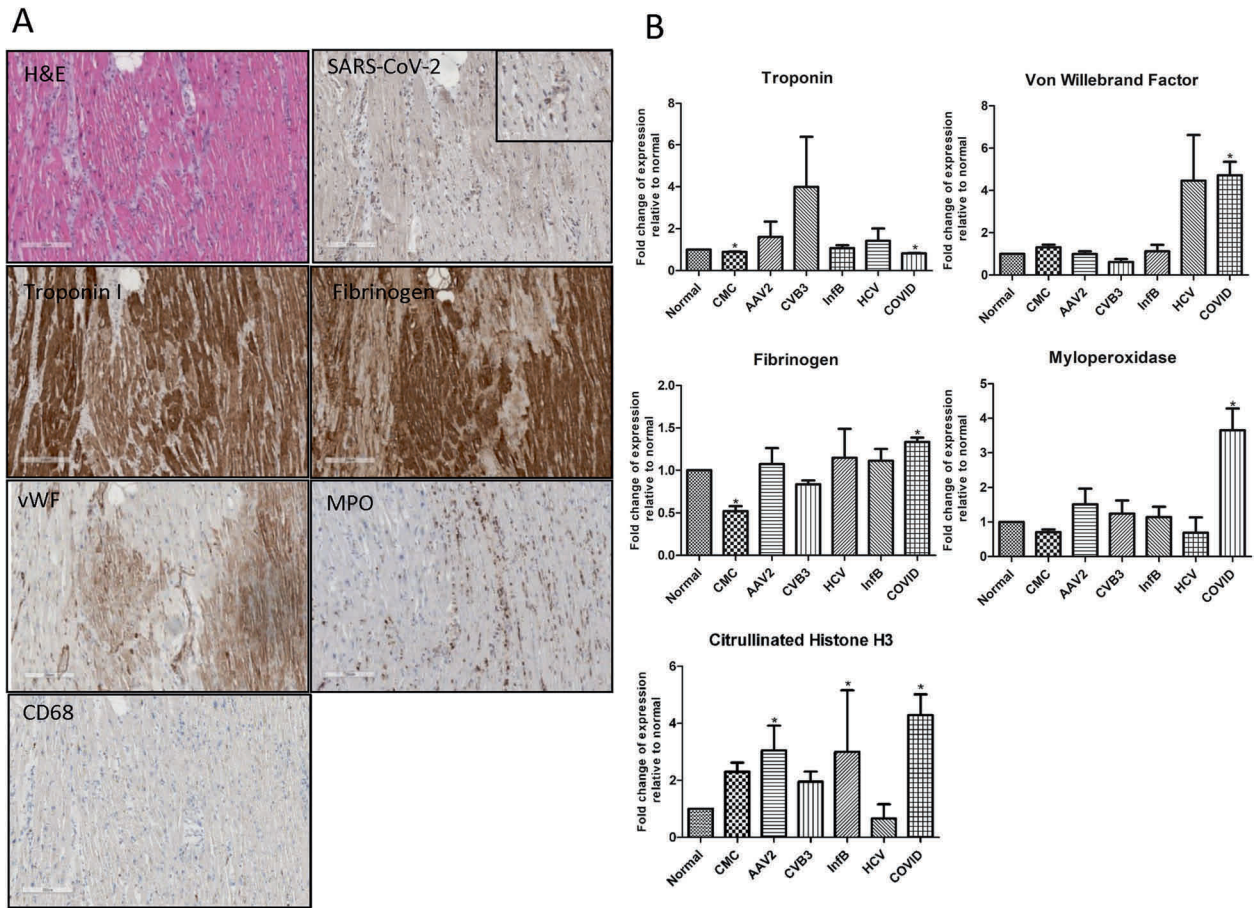
Fig. 4 Abundant myocardial damage in the absence of detectable virus in a critically ill COVID-19 patient. A Characteristic section from the left ventricle of a COVID-19-positive decedent. Cardiomyocyte structural protein troponin-I (brown) is depleted in regions of injury in regions of fibrinogen (brown) and vWF (brown) deposition. Diffuse myeloperoxidase (MPO) staining (brown), indicative of neutrophil extracellular traps (NETs), are prominent in the interstitial spaces in the same region of myocyte damage (MPO, brown). All images are at ×10 magnification within the same region. **B** Graphical representation of troponin-I, fibrinogen, vWF, and myeloperoxidase (MPO) expression in the hearts of COVID-19 patients compared to normal, clinically matched control (CMC), HCV-, influenza B-, AAV2- and CVB3-positive heart failure patients. Sample size were as followed: normal ($n = 10$); CMC ($n = 14$); viral myocarditis ($n = 12$: AAV2 ($n = 3$); CVB3 ($n = 3$); Inf B ($n = 3$); HCV ($n = 3$)); COVID ($n = 21$). *denotes statistical significance relative to normal control heart tissue ($p < 0.05$).

associated with intracellular SARS-CoV-2 viral presence and disruption of the endothelial cell membranes, and overall wide-spread thrombosis with microangiopathy[37]. Increased circulatory markers of angiogenesis have also been observed in severe cases of COVID-19[38], aligning with our reports of significantly increased levels of CD31 in cardiac tissue unique to COVID-19 relative to all other virus-associated heart failure (2.12-fold increase). Others have reported similar associations between thrombosis and the novel coronavirus disease[5]. Al-Samkari et al., for example, noted an overall thrombotic complication rate of 9.5% (45 events in 38 COVID-19 patients)[39]. Here we report thrombosis in 19.1% (4/21) COVID-19-positive decedents.

Arterial thrombosis, in particular, leading to stroke or myocardial infarction, is reported to have occurred in up to 4% of COVID-19 patients in intensive care[40]. In addition, autopsy studies on COVID-19 decedents have noted prominent endothelial inflammation and microvascular thrombosis with inflammatory cells found attached to the endothelium of small vessels in the heart[40], further demonstrated in our cohort (Figs. 3 and 5). This may be explained by the fact that endothelial dysfunction plays a role in microvascular thrombosis, secondary to the amplified inflammatory response triggered in SARS-CoV-2-infected patients. We report evidence of endothelial damage with significantly elevated levels of vWF and fibrinogen in our COVID-19 cohort, which are hypothesized to result in uncontrolled hypercoagulability. The

presence of thrombi in vascular beds of the heart is associated with hypoxia-induced vWF upregulation[41]. Others have observed elevated levels of vWF in blood samples from COVID-19 patients[42,43], and one group observed factor VIII, a glycoprotein closely linked to vWF, in COVID-19-positive cardiac autopsy tissue that was indicative of nonocclusive fibrin microthrombi[44]. However, this is the largest study to date to detect vWF specifically in the heart of COVID-19 patients in thrombi and surrounding vasculature (Fig. 5), as well as in the myocardium in regions of fibrotic remodeling (Fig. 4). VWF levels were found to be high in COVID-19 ICU patients as compared to other septic ICU patients[45], which is reflected in our COVID-19 cohort compared to non-virus infected controls (3.59-fold increase) and all virus-associated heart failure controls (3.03-fold increase mean), suggesting a COVID-19 specific process. VWF is additionally hypothesized to be a prognostic measure of thrombotic risk in COVID-19 patients and contributes to disease severity[46].

Moreover, complement activation is shown to contribute to endothelial cell dysfunction and exocytosis of vWF and platelet proteins, which causes prothrombinase activity and micro-thrombogenesis[47–49]. This, in turn, results in cardiac dysfunction. Our findings of increased complement protein C4D (4.44-fold relative to CMC) align with a recent study by Pellegrini et al. on the hearts of 40 COVID-positive decedents, which demonstrated that myocyte necrosis was caused by microthrombi and showed
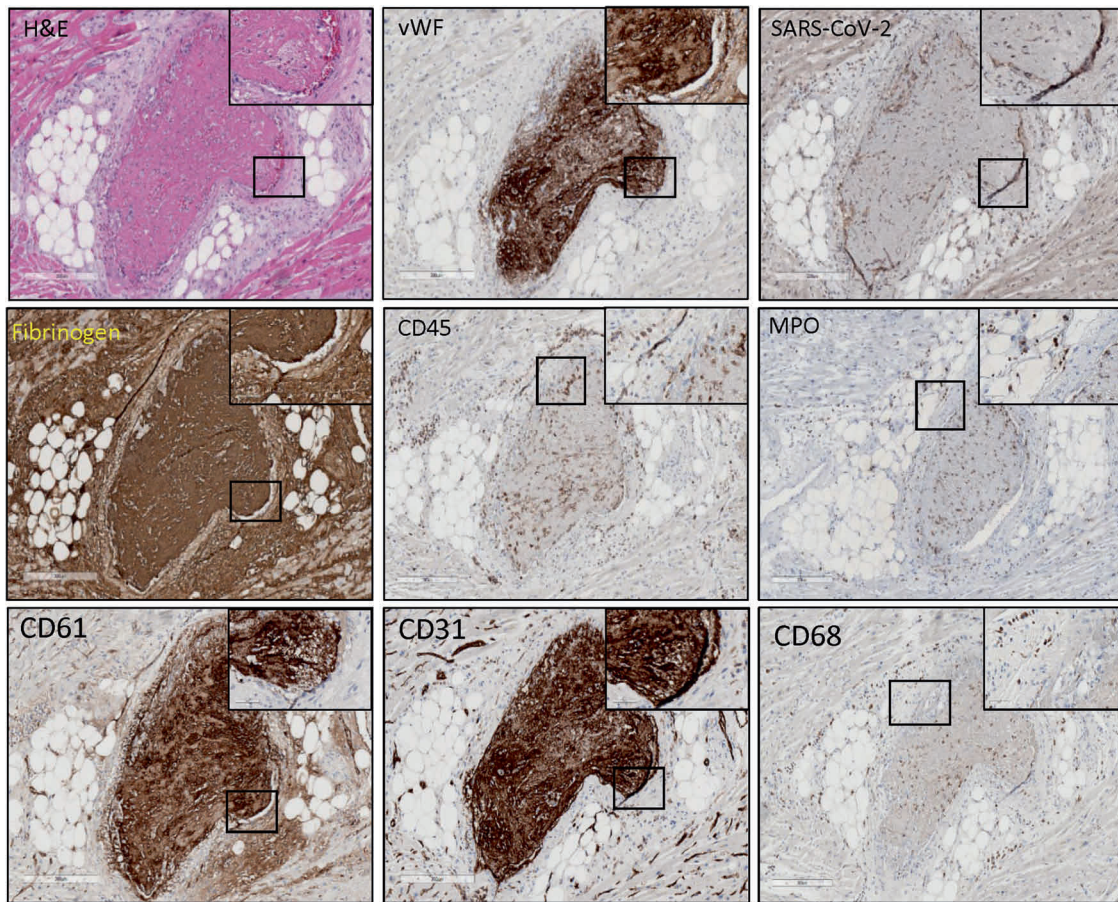
Fig. 5   SARS-CoV-2 infection of the endothelium, resultant damage, and thrombosis as a defining feature in COVID-19-associated cardiac injury. A large characteristic thrombus (750–100 μm) penetrating an artery within the myocardium of a COVID-19-positive decedent was reported. SARS-CoV-2 spike protein was prominently expressed (brown) in the endothelium. Neutrophil extracellular traps (NETs) were interspersed throughout as indicated by myeloperoxidase (MPO) (brown) within the thrombus and in the artery wall near the endothelial-thrombus interface. Archetypical expression of vWF (brown) indicative of endothelial injury is prominent in the lining of the elastica and along with fibrinogen (brown) forms the thrombus. CD45 (leukocyte common antigen) (brown) demonstrates prominent inflammation within the thrombus and surrounding vasculature. H&E indicates hematoxylin and eosin staining. Images are shown at ×10 magnification, with inserts shown at ×40 magnification.

higher fibrin and C5b-9 complement expression when compared to intramyocardial thromboemboli from non-COVID-19-infected individuals[50].

NETs, which we report at significant levels in all COVID-19 patients in our cohort as indicated by MPO staining and 18/21 patients by CitH3 staining[51,52], are involved in the exacerbation of various disease processes (such as diabetes, obesity, and deep vein thrombosis[53]) that are associated with increased morbidity and mortality related to COVID-19[54,55]. As such, NETs activate the coagulation complement pathway, amplify inflammatory processes and are associated with the pathogenesis of arterial and venous thrombosis[17]. In the context of COVID-19, previous studies have demonstrated NETs as being involved in thrombus formation, fibrosis, and inflammation-associated damage[56]. It has also been demonstrated that sera from patients with COVID-19 have elevated MPO-DNA and citrullinated histone H3 (CitH3), markers of NETs[57]. The observation of higher MPO-DNA and CitH3 in patients receiving mechanical ventilation compared to those without the need of oxygen supplementation indicates a correlation between NETs, which has been documented in the lungs of COVID-19 patients[56], and disease severity, which is corroborated by our study with 95.2% (20/21) patients receiving mechanical ventilation (see Supplementary Table 1A). In the present study, MPO was found to be substantially upregulated in COVID-19 patients relative to all other forms of virus-related

heart failure, which indicates a process unique to COVID-19 pathogenesis—this points toward NETs as a potential therapeutic target. We found MPO to be expressed transmurally that included thrombi (Fig. 5), areas of fibrotic remodeling of the myocardium (Fig. 4), and myocarditic lesions (Supplementary Fig. 2) within our cohort. Thus, NETs may be a distinguishing factor linking the hypercoagulative, prothrombotic state to the hyperinflammatory cytokine storm described in some critically ill COVID-19 patients[58].

We also provide further evidence that SARS-CoV-2 infection evokes inflammatory immune responses, responsible for a cytokine storm and thus leads to critical disease. Indirect ischemic cardiac injury due to direct damage to the lungs in COVID-19 patients may have triggered the immune cell infiltration observed in the hearts of most patients in our cohort. Following the initial response of neutrophils homing to the cardiac tissue after ischemic injury, IL-6 is produced and recruits macrophages to the myocardium[58]. In Basso et al.'s study of 21 COVID-19 autopsies, it was determined that 86% of patients had increased macrophage presence in the myocardial interstitium[59]. Another autopsy study reported high expression of macrophages in the myocardium of COVID-19 decedents[60], which is reflected in our cohort as seen in the upregulation in IL-6 and macrophage (CD68) expression in comparison to healthy hearts and CMC (Fig. 6 and Supplementary Fig. 1).
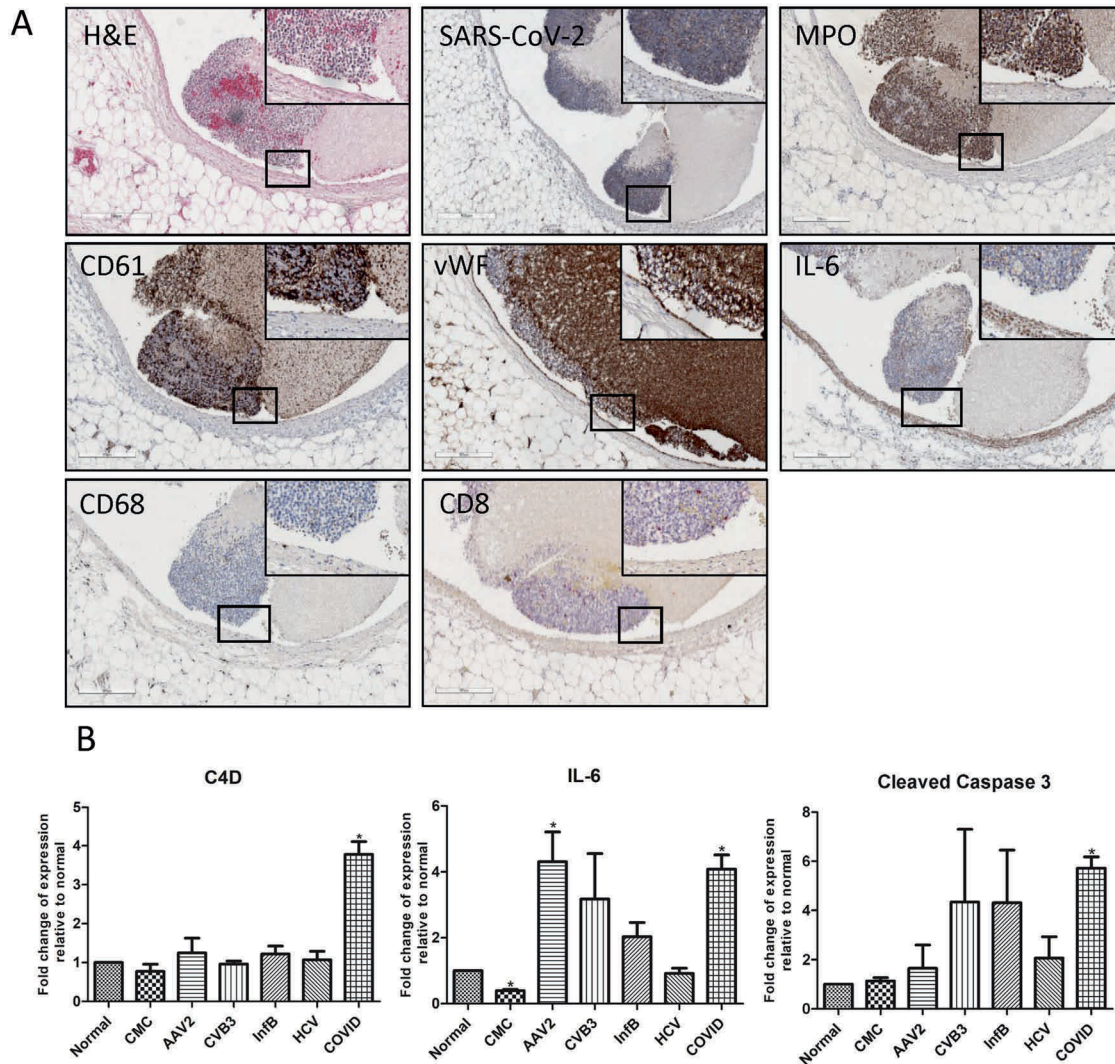
Fig. 6 Luminal collection of mixed lymphoid cells along the right ventricular septum of an acutely ill COVID-19 patient. A A large mass of leukocytes consisting of predominantly neutrophils (myeloperoxidase (MPO)), with rare macrophage, CD8, and CD4 positive T cells. Rare, focal SARS-CoV-2 replicating (CoV-19S) strand positive cell (yellow arrow) was detected within the mass and focally within the surrounding myocardium via RNAscope®. IL-6 was detected within the mass and surrounding endocardium and myocardium (brown). CD61-positive cells (brown) were interspersed diffusely throughout the inflammatory cell mass. **B** Graphical representation of C4D, IL-6, caspase-3 expression quantified in Aperio ImageScope software. Sample size were as followed: normal ($n = 10$); CMC ($n = 14$); viral myocarditis ($n = 12$: AAV2 ($n = 3$); CVB3 ($n = 3$); Inf B ($n = 3$); HCV ($n = 3$)); COVID ($n = 21$). *denotes statistical significance relative to normal control heart tissue ($p < 0.05$).

Among the many modalities by which COVID-19 has been demonstrated to affect the heart, myocarditis has been reported in the critically ill patients, in children associated with MIS-C, in adults (manifesting as post-acute infection), and in previously asymptomatic individuals where clinical presentation may mimic a heart attack and is attributed to sudden death[3,61]. To date, reports on the frequency and severity of COVID-19-associated myocarditis have been highly variable. Estimates from a recent meta-analysis reported myocarditis in only 7.2% of decedents, while others have reported myocarditis in 60% of patients surveyed[62]. Incidence has widely varied among published cohorts, reflecting the uncertainty and gaps in knowledge surrounding COVID-19-associated cardiac injury[62]. Within our patient cohort, 19 of 21 patients were diagnosed with borderline myocarditis at autopsy, meeting the histopathologic definition put forth in the Dallas criteria. Myocarditis among our patient cohort was typically concurrent with vasculitis, thrombosis, and ischemic damage. Additional features of cardiovascular injury, including edema (90% of patients), myocyte hypertrophy (71%), and myocytolysis (48%)

were commonly noted, although fibrosis (43%) and hemorrhage (19%) were also present (see Supplementary Table 1B). In patients with borderline myocarditis, we observed mixed but predominantly mononuclear inflammatory infiltrates consisting of neutrophils, macrophages, and, lymphocytes, which were predominantly CD4- with sparse CD8-positive T cells (Fig. 5).

While many studies report a decrease in serum lymphocyte presence (lymphopenia)[63], the presence of lymphocytes in the myocardium of COVID-19 patients has not been extensively examined. However, it has been determined that CD4+ cells play a pathological role in heart failure severity by supporting a pro-inflammatory response that further promotes cardiac remodeling[58]. An autopsy study of COVID-19 decedents reports increased CD4+ T cell expression in the myocardium of all patients[60]. Similarly, in our cohort, the significant increase in CD4+ T cell presence in COVID-19 patient myocardium as compared to control patients aligns with severe cardiac damage. Our reports of decreased CD8 expression align with Urra et al.'s findings of reduced CD8 cell levels in the blood as a marker of worse
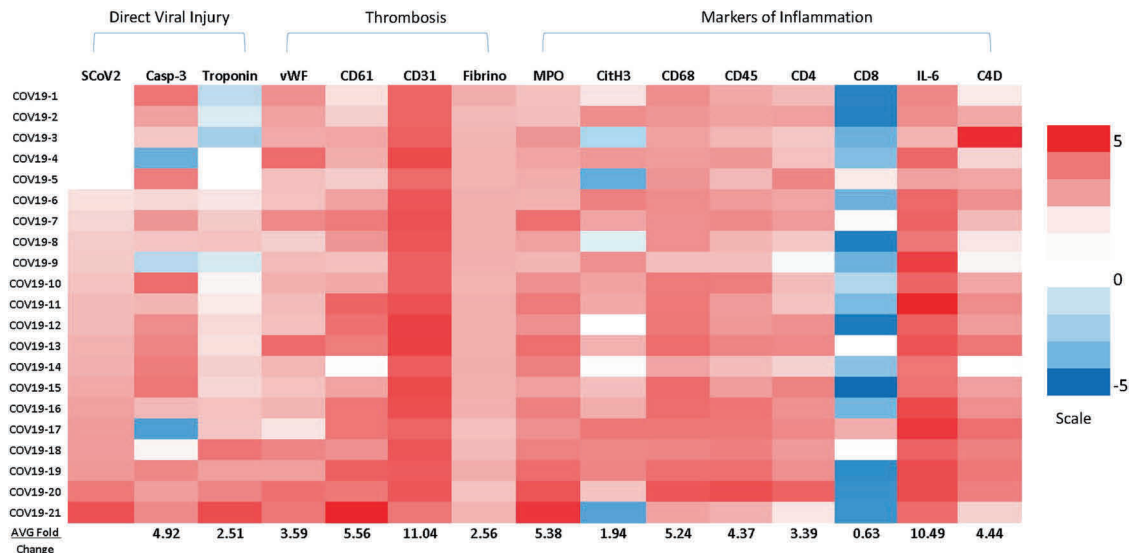
Fig. 7 Heatmap of markers of direct and indirect SARS-CoV-2-associated myocardial injury COVID-19-positive patients. The relative intensity of the indicated markers stained via immunohistochemistry and quantified using computer-aided image analysis. All values were normalized to the average signal intensity of clinically matched controls. Red indicates higher expression; blue indicates lower than normal expression. COVID-19 patients were arranged based on quantification of SARS-CoV-2 from lowest to highest signal. Average signal quantification for each protein marker is shown at the bottom of each column. The heatmap is divided into direct viral injury and indirect injury (i.e., thrombosis or markers of inflammation).

prognosis and increased inflammation in COVID-19 patients[64]. A higher CD4:CD8 ratio has been correlated with poorer disease outcomes[65], consistent with our results (Fig. 7).

Within our comparison of COVID-19 patients to CMC, the only notable differentiation between the groups appears to be SARS-CoV-2 infection. By eliminating variability in age, sex, BMI, and various comorbidities to the extent of our resources, it can be further supported that significant differences in protein expression are unique to SARS-CoV-2 infection and independent of the external factors previously mentioned.

This study is, to our knowledge, the first of its kind in which there was a performance of in-depth IHC analyses juxtaposed with corresponding patient clinical history and pathological reports, effectively charting the course of the novel disease relative to all currently postulated mechanisms of COVID-19-associated cardiac injury. This study also provides spatial context and quantitative proteomic insights into the nature of SARS-CoV-2-associated cardiac injury in COVID-19 patients. We anticipate our findings will contribute to delineating the unique mechanisms of SARS-CoV-2-associated cardiac injury while identifying commonalities among protein expression between COVID-19, controls, and other forms of virus-associated heart failure. Notably, COVID-19 heart damage was primarily indirect in nature, with inflammation occurring typically in and around sites of thrombus formation and regions of ischemia, with sparse regions of viral positivity. In other etiologies of virus-associated heart failure, myocarditis associated with direct viral injury was the defining feature; NETs (MPO)-associated injury and inflammation, with enhanced thrombosis and vasculitis, appear to be a defining feature of COVID-19-associated cardiac injury, further demonstrated by a correlation between NETs and SARS-CoV-2 expression. Our findings suggest that COVID-19-associated heart damage is multifactorial (attributable to direct viral damage, thrombotic damage in a hypercoagulative state, and aberrant cytokine- and immune cell-mediated damage—the latter likely being a consequence of a hypercoagulative state mediated by endothelialitis and vascular thrombosis triggering dysregulated immune responses).

Moreover, we identified protein markers involved in direct and indirect mechanisms of cardiac injury such as vWF and MPO, which may serve as distinguishing factors linking the phases of injury observed in critically ill COVID-19 patients. These phases are enhanced by many of the underlying conditions (i.e., obesity, diabetes, and hypertension) that render such individuals more vulnerable to severe outcomes and poor prognosis. VWF and NETs may serve as potential candidates for prognostic, diagnostic, and therapeutic guidance regarding to COVID-19-associated heart failure. The spectrum of injury reported among our small patient cohort supports the notion that further investigation into the mechanisms of COVID-19-associated cardiac injury in larger patient populations is warranted.

Limitations

Our study was limited by the number of normal and viral myocarditis patients who were available to use. Utilizing all of the hearts in our research center that were diagnosed with viral myocarditis, we performed in situ hybridization to determine the etiology of myocarditis that resulted in three each of CVB3, AAV2, influenza B, and HCV. Furthermore, cleaved caspase-3 is suggestive, but not a specific indicator for direct viral injury, as indirect effects of the viral injury may also contribute to increased cleaved caspase-3 expression. Cleaved caspase-3 remains also to be suggestive of apoptosis, as the gold standard is electron microscopy. Another limitation of the study was the histopathologic diagnosis of borderline myocarditis. In this manuscript, the guidelines of the Dallas criteria for myocarditis were followed although tools including cardiovascular magnetic resonance imaging are complementary in obtaining a complete diagnosis. Despite using the current gold standard, all patients were diagnosed post-mortem and thus the pathological and IHC analysis of formalin-fixed paraffin-embedded cardiac tissue sections were the only methods available and may have limited the accuracy of diagnoses.

824

REFERENCES

1. Knowlton, K. U. Pathogenesis of SARS-CoV-2 induced cardiac injury from the perspective of the virus. *J. Mol. Cell Cardiol.* **147**, 12–17 (2020).
2. Shi, S., Qin, M., Shen, B., Cai, Y., Liu, T., Yang, F. et al. Association of cardiac injury with mortality in hospitalized patients with COVID-19 in Wuhan, China. *JAMA Cardiol.* **5**, 802–810 (2020).
3. Puntmann, V. O., Carerj, M. L., Wieters, I., Fahim, M., Arendt, C. & Hoffmann, J. et al. Outcomes of cardiovascular magnetic resonance imaging in patients recently recovered from coronavirus disease 2019 (COVID-19). *JAMA Cardiol.* **5**, 1265–1273 (2020).
4. Choudry, F. A., Hamshere, S. M., Rathod, K. S., Akhtar, M. M., Archbold, R. A. & Guttmann, O. P. et al. High thrombus burden in patients with COVID-19 presenting with ST-segment elevation myocardial infarction. *J. Am. Coll. Cardiol.* **76**, 1168–1176 (2020).
5. Rapkiewicz, A. V., Mai, X., Carsons, S. E., Pittaluga, S., Kleiner, D. E. & Berger, J. S. et al. Megakaryocytes and platelet-fibrin thrombi characterize multi-organ thrombosis at autopsy in COVID-19: a case series. *EClinicalMedicine* **24**, 100434 (2020).
6. Kuck, K. H. Arrhythmias and sudden cardiac death in the COVID-19 pandemic. *Herz* **45**, 325–326 (2020).
7. Zheng, Y.-Y., Ma, Y.-T., Zhang, J.-Y. & Xie, X. COVID-19 and the cardiovascular system. *Nat. Rev. Cardiol.* **17**, 259–260 (2020).
8. Mehra, M. R., Desai, S. S., Kuy, S., Henry, T. D., & Patel, A. N. Cardiovascular disease, drug therapy, and mortality in COVID-19. *N. Engl. J. Med.* **382**, e102 (2020).
9. Madjid, M., Safavi-Naeini, P., Solomon, S. D., & Vardeny, O. Potential effects of coronaviruses on the cardiovascular system: a review. *JAMA Cardiol.* **5**, 831–840 (2020).
10. Guo, T., Fan, Y., Chen, M., Wu, X., Zhang, L., He, T. et al. Cardiovascular implications of fatal outcomes of patients with coronavirus disease 2019 (COVID-19). *JAMA Cardiol.* **5**, 811–818 (2020).
11. Belhadjer, Z., Méot, M., Bajolle, F., Khraiche, D., Legendre, A., Abakka, S. et al. Acute heart failure in multisystem inflammatory syndrome in children (MIS-C) in the context of global SARS-CoV-2 pandemic. *Circulaion* **142**, 429–436 (2020).
12. Guzik, T. J., Mohiddin, S. A., Dimarco, A., Patel, V., Savvatis, K. & Marelli-Berg, F. M. et al. COVID-19 and the cardiovascular system: implications for risk assessment, diagnosis, and treatment options. *Cardiovasc. Res.* **116**, 1666–1687 (2020).
13. Lindner, D., Fitzek, A., Bräuninger, H., Aleshcheva, G., Edler, C., Meissner, K. et al. Association of cardiac infection with SARS-CoV-2 in confirmed COVID-19 autopsy cases. *JAMA Cardiol.* **5**, 1281–1285 (2020).
14. Tersalvi, G., Vicenzi, M., Calabretta, D., Biasco, L., Pedrazzini, G., & Winterton, D. Elevated troponin in patients with coronavirus disease 2019 (COVID-19): possible mechanisms. *J. Card. Fail.* **26**, 470–475 (2020).
15. Giannis, D., Ziogas, I. A., & Gianni, P. Coagulation disorders in coronavirus infected patients: COVID-19, SARS-CoV-1, MERS-CoV and lessons from the past. *J. Clin. Virol.* **127**, 104362 (2020).
16. Bikdeli, B., Madhavan, M. V., Jimenez, D., Chuich, T., Dreyfus, I. & Driggin, E. et al. COVID-19 and thrombotic or thromboembolic disease: implications for prevention, antithrombotic therapy, and follow-up: JACC state-of-the-art review. *J. Am. Coll. Cardiol.* **75**, 2950–2973 (2020).
17. Shi, S. Y., Zhou, Q., He, Z. Q., Shen, Z. F., Zhang, W. X. & Zhang, D. et al. Traditional Chinese medicine (Liang-Xue-Di-Huang Decoction) for hemorrhoid hemorrhage: Study Protocol Clinical Trial (SPIRIT Compliant). *Medicine (Baltimore)* **99**, e19720 (2020).
18. Moore, J. B. & June, C. H. Cytokine release syndrome in severe COVID-19. *Science* **368**, 473–474 (2020).
19. Perez-Bermejo, J. A., Kang, S., Rockwood, S. J., Simoneau, C. R., Joy, D. A., Silva, A. C. et al. SARS-CoV-2 infection of human iPSC-derived cardiac cells reflects cytopathic features in hearts of patients with COVID-19. *Sci. Transl. Med.* **13**, eabf7872 (2021).
20. Nicin, L., Abplanalp, W. T., Mellentin, H., Kattih, B., Tombor, L. & John, D. et al. Cell type-specific expression of the putative SARS-CoV-2 receptor ACE2 in human hearts. *Eur* **41**, 1804–1806 (2020).
21. Verdecchia, P., Cavallini, C., Spanevello, A., & Angeli F. The pivotal link between ACE2 deficiency and SARS-CoV-2 infection. *Eur. J. Intern. Med.* **76**, 14–20 (2020).
22. Aguiar, J. A., Tremblay, B. J., Mansfield, M. J., Woody, O., Lobb, B., Banerjee, A. et al. Gene expression and in situ protein profiling of candidate SARS-CoV-2 receptors in human airway epithelial cells and lung tissue. *Eur. Respir. J.* **56**, 2001123 (2020).
23. Yang, L., Han, Y., Nilsson-Payant, B. E., Gupta, V., Wang, P. & Duan, X. et al. A human pluripotent stem cell-based platform to study SARS-CoV-2 tropism and model virus infection in human cells and organoids. *Cell Stem Cell* **27**, 125–36.e7 (2020).
24. McFadyen, J. D., Stevens, H. & Peter, K. The emerging threat of (micro) thrombosis in COVID-19 and its therapeutic implications. *Circ. Res.* **127**, 571–587 (2020).
25. Wichmann, D., Sperhake, J.-P., Lütgehetmann, M., Steurer, S., Edler, C., Heinemann, A. et al. Autopsy findings and venous thromboembolism in patients with COVID-19: a prospective cohort study. *Ann. Intern. Med.* **173**, 268–277 (2020).
26. Akhmerov, A. & Marbán, E. COVID-19 and the heart. *Circ. Res.* **126**, 1443–1455 (2020).
27. Hadjadj, J., Yatim, N., Barnabei, L., Corneau, A., Boussier, J. & Smith, N. et al. Impaired type I interferon activity and inflammatory responses in severe COVID-19 patients. *Science* **369**, 718–724 (2020).
28. Schurink, B., Roos, E., Radonic, T., Barbe, E., Bouman, C. S., de Boer, H. H. et al. Viral presence and immunopathology in patients with lethal COVID-19: a prospective autopsy cohort study. *Lancet Microbe.* **1**, e290–e299 (2020).
29. Leisman, D. E., Ronner, L., Pinotti, R., Taylor, M. D., Sinha, P., Calfee, C. S. et al. Cytokine elevation in severe and critical COVID-19: a rapid systematic review, meta-analysis, and comparison with other inflammatory syndromes. *Lancet Respir. Med.* **8**, 1233–1244 (2020).
30. Goshua, G., Pine, A. B., Meizlish, M. L., Chang, C.-H., Zhang, H. & Bahel, P. et al. Endotheliopathy in COVID-19-associated coagulopathy: evidence from a single-centre, cross-sectional study. *Lancet Haematol.* **7**, e575–e582 (2020).
31. Bulfamante, G. P., Perrucci, G. L., Falleni, M., Sommariva, E., Tosi, D., Martinelli, C. et al. Evidence of SARS-CoV-2 transcriptional activity in cardiomyocytes of COVID-19 patients without clinical signs of cardiac involvement. *Biomedicines* **8**, 626 (2020).
32. Roshdy, A., Zaher, S., Fayed, H., & Coghlan, J. G. COVID-19 and the heart: a systematic review of cardiac autopsies. *Front. Cardiovasc. Med.* **7**, 626975 (2021).
33. Cinti, S., Graciotti, L., Giordano, A., Valerio, A., & Nisoli, E. COVID-19 and fat embolism: a hypothesis to explain the severe clinical outcome in people with obesity. *Int. J. Obes.* **44**, 1800–1802 (2020).
34. Gupte, M., Boustany-Kari, C. M., Bharadwaj, K., Police, S., Thatcher, S. & Gong, M. C. et al. ACE2 is expressed in mouse adipocytes and regulated by a high-fat diet. *Am. J. Physiol. Regul. Integr. Comp. Physiol.* **295**, R781–R788 (2008).
35. Kassir, R. Risk of COVID-19 for patients with obesity. *Obes. Rev.* **21**, e13034 (2020).
36. Cai, Q., Chen, F., Wang, T., Luo, F., Liu, X., Wu, Q. et al. Obesity and COVID-19 severity in a designated hospital in Shenzhen, China. *Diabetes Care* **43**, 1392–1398 (2020).
37. Ackermann, M., Verleden, S. E., Kuehnel, M., Haverich, A., Welte, T., Laenger, F. et al. Pulmonary vascular endothelialitis, thrombosis, and angiogenesis in Covid-19. *N. Engl. J. Med.* **383**, 120–128 (2020).
38. Pine, A. B., Melizlish, M. L., Goshua, G., Chang C.-H., Zhang H., Bishai J. et al. Circulating markers of angiogenesis and endotheliopathy in COVID-19. *Pulm. Circ.* **10**, 2045894020966547 (2020).
39. Al-Samkari, H., Karp Leaf, R. S., Dzik, W. H., Carlson, J. C., Fogerty, A. E. & Waheed, A. et al. COVID-19 and coagulation: bleeding and thrombotic manifestations of SARS-CoV-2 infection. *Blood* **136**, 489–500 (2020).
40. Lowenstein, C. J., & Solomon, S. D. Severe COVID-19 is a microvascular disease. *Circulation* **142**, 1609–1611 (2020).
41. Mojiri, A., Alavi, P., Carrillo, M. A. L., Nakhaei-Nejad, M., Sergi, C. M. & Thebaud, B. et al. Endothelial cells of different organs exhibit heterogeneity in von Willebrand factor expression in response to hypoxia. *Atherosclerosis* **282**, 1–10 (2019).
42. Helms, J., Tacquard, C., Severac, F., Leonard-Lorant, I., Ohana, M., Delabranche, X. et al. High risk of thrombosis in patients with severe SARS-CoV-2 infection: a multicenter prospective cohort study. *Intensive Care Med.* **46**, 1089–1098 (2020).
43. Cipolloni, L., Sessa, F., Bertozzi, G., Baldari, B., Cantatore, S. & Testi, R. et al. Preliminary post-mortem COVID-19 evidence of endothelial injury and factor VIII hyperexpression. *Diagnostics* **10**, 575 (2020).
44. Bois, M. C., Boire, N. A., Layman, A. J., Aubry, M.-C., Alexander, M. P. & Roden, A. C. et al. COVID-19–associated nonocclusive fibrin microthrombi in the heart. *Circulation* **143**, 230–243 (2021).
45. Vassiliou, A. G., Keskinidou, C., Jahaj, E., Gallos, P., Dimopoulou, I. & Kotanidou, A. et al. ICU admission levels of endothelial biomarkers as predictors of mortality in critically ill COVID-19 patients. *Cells* **10**, 186 (2021).
46. Ladikou, E. E., Sivaloganathan, H., Milne, K. M., Arter, W. E., Ramasamy, R. & Saad, R. et al. Von Willebrand factor (vWF): marker of endothelial damage and thrombotic risk in COVID-19? *Clin. Med.* **20**, e178 (2020).
47. Hendaus, M. A., & Jomha, F. A. From COVID-19 to clot: the involvement of the complement system. *J. Biomol. Struct. Dyn.* **40**, 1909–1914 (2020).
48. Skendros, P., Mitsios, A., Chrysanthopoulou, A., Mastellos, D. C., Metallidis, S. & Rafailidis, P. et al. Complement and tissue factor–enriched neutrophil extracellular traps are key drivers in COVID-19 immunothrombosis. *J. Clin. Investig.* **130**, 6151–6157 (2020).
49. Campbell, C. M. & Kahwash, R. Will complement inhibition be the new target in treating COVID-19–related systemic thrombosis? *Circulation* **141**, 1739–1741 (2020).
50. Pellegrini, D., Kawakami, R., Guagliumi, G., Sakamoto, A., Kawai, K., Gianatti, A. et al. Microthrombi as a major cause of cardiac injury in COVID-19: a pathologic study. *Circulation* **143**, 1031–1042 (2021).

51. Papayannopoulos, V., Metzler, K. D., Hakkim, A. & Zychlinsky, A. Neutrophil elastase and myeloperoxidase regulate the formation of neutrophil extracellular traps. *J. Cell Biol.* **191**, 677–691 (2010).

52. Metzler, K. D., Goosmann, C., Lubojemska, A., Zychlinsky, A. & Papayannopoulos, V. A myeloperoxidase-containing complex regulates neutrophil elastase release and actin dynamics during NETosis. *Cell Rep.* **8**, 883–896 (2014).

53. Delgado-Rizo, V., Martínez-Guzmán, M. A., Iñiguez-Gutierrez, L., García-Orozco, A., Alvarado-Navarro, A. & Fafutis-Morris, M. Neutrophil extracellular traps and its implications in inflammation: an overview. *Front. Immunol.* **8**, 81 (2017).

54. Santoliquido, A., Porfidia, A., Nesci, A., De Matteis, G., Marrone, G. & Porceddu, E. et al. Incidence of deep vein thrombosis among non-ICU patients hospitalized for COVID-19 despite pharmacological thromboprophylaxis. *J. Thromb. Haemost.* **18**, 2358–2363 (2020).

55. Sattar, N., McInnes, I. B., & McMurray, J. J. Obesity a risk factor for severe COVID-19 infection: multiple potential mechanisms. *Circulation* **142**, 4–6 (2020).

56. Radermecker, C., Detrembleur, N., Guiot, J., Cavalier, E., Henket, M., d'Emal, C. et al. Neutrophil extracellular traps infiltrate the lung airway, interstitial, and vascular compartments in severe COVID-19. *J. Exp. Med.* **217**, e20201012 (2020).

57. Zuo, Y., Yalavarthi, S., Shi, H., Gockman, K., Zuo, M., Madison, J. A. et al. Neutrophil extracellular traps in COVID-19. *JCI Insight* **5**, e138999 (2020).

58. Unudurthi, S. D., Luthra, P., Bose, R. J., McCarthy, J., & Kontaridis, M. I. Cardiac inflammation in COVID-19: lessons from heart failure. *Life Sci.* **260**, 118482 (2020).

59. Basso, C., Leone, O., Rizzo, S., De Gaspari, M., van der Wal, A. C. & Aubry, M.-C. et al. Pathological features of COVID-19-associated myocardial injury: a multicentre cardiovascular pathology study. *Eur. Heart J.* **41**, 3827–3835 (2020).

60. Yao, X., Li, T., He, Z., Ping, Y., Liu, H. & Yu, S. et al. A pathological report of three COVID-19 cases by minimally invasive autopsies. *Zhonghua Bing Li Xue Za Zhi* **49**, 411–417 (2020).

61. Hudowenz, O., Klemm, P., Lange, U., Rolf, A., Schultheiss, H.-P., Hamm, C. et al. Case report of severe PCR-confirmed COVID-19 myocarditis in a European patient manifesting in mid January 2020. *Eur. Heart J.* **4**, 1–6 (2020).

62. Halushka, M. K., & Vander Heide, R. S. Myocarditis is rare in COVID-19 autopsies: cardiovascular findings across 277 post-mortem examinations. *Cardiovasc. Pathol.* **50**, 107300 (2020).

63. Huang, I. & Pranata, R. Lymphopenia in severe coronavirus disease-2019 (COVID-19): systematic review and meta-analysis. *J. Intensive Care* **8**, 1–10 (2020).

64. Urra, J., Cabrera, C., Porras, L. & Ródenas, I. Selective CD8 cell reduction by SARS-CoV-2 is associated with a worse prognosis and systemic inflammation in COVID-19 patients. *Clin. Immunol.* **217**, 108486 (2020).

65. Pallotto, C., Suardi, L. R., Esperti, S., Tarquini, R., Grifoni, E., Meini, S. et al. Increased CD4/CD8 ratio as a risk factor for critical illness in coronavirus disease 2019 (COVID-19): a retrospective multicentre study. *J. Infect. Dis.* **52**, 675–677 (2020).

ACKNOWLEDGEMENTS

AUTHOR CONTRIBUTIONS
P.J.H., F.L.-F., T.A.M., C.N., A.R.H., and R.C. performed study concept and design; P.J.H., F.L.-F., T.A.M., C.L., C.N., A.R.H., R.C., B.G., H.R., J.H., D.R.A., S.J.R., and B.M.M. performed development of methodology and writing, review and revision of the paper; P.J.H., F. L.-F., T.A.M., C.L., C.N., A.R.H., B.G., S.J.R., and B.M.M. provided acquisition, analysis and interpretation of data, and statistical analysis; P.J.H., B.G., S.J.R., and B.M.M. provided technical and material support. All authors read and approved the final paper.

FUNDING

COMPETING INTERESTS
The authors declare no competing interests.

ETHICS APPROVAL
Ethics protocols (H05-50004, H15-40080) approved by the University of British Columbia's Clinical Research Ethics Board were followed. This study was performed in accordance with the Declaration of Helsinki.

ADDITIONAL INFORMATION
Supplementary information The online version contains supplementary material available at https://doi.org/10.1038/s41374-022-00783-x.

Correspondence and requests for materials should be addressed to Paul J. Hanson.

Reprints and permission information is available at http://www.nature.com/reprints

Publisher's note Springer Nature remains neutral with regard to jurisdictional claims in published maps and institutional affiliations.